Available online at www.sciencedirect.com

ScienceDirect

Physics Procedia 5 (2010) 439–448

Physics Procedia

www.elsevier.com/locate/procedia

LANE 2010

Laser surface treatment of grey cast iron by high power diode laser

Anmin Liu[a]*, Barbara Previtali[a]

[a]*Politecnico di Milano, Dipartimento di Meccanica, Via La Masa 1, 20156 Milan, Italy*

Abstract

A grey cast iron surface was heat treated by a 1kW diode laser to improve the hardness and wear resistance of the surface. Based on a temperature measurement and control system, different levels of surface temperature and scan speed were investigated for single and multi-pass hardening processes. A homogeneous hardened zone with hardness 700-800 HV0.3 was obtained in cross section regardless to the process temperature and scan speed during single pass laser hardening. Considering the process productivity, the optimal combination of high temperature and high scan speed was used to identify the process condition to be used in the multi-pass laser hardening. The selected parameters were then applied in large surface treatment to investigate the effect of the overlapping procedure on the surface properties. Different overlapping lengths were investigated to produce a large hardened area with uniform hardening depth and hardness.

Keywords: Grey cast iron; laser surface treatment; microstructure; microhardness; overlapping

1. Introduction

Grey cast iron is widely used in components such as pistons, guides, valves, tool beds; due to its good properties, such as excellent machinability and castability, as well as low price [1]. Surface treatment is usually applied to improve hardness, wear resistance and also corrosion properties on the material surface of cast iron components to meet the high performance and reliability of industrial requirements such as high load and high pressure [2-4].

Laser hardening is a promising process for the ferrous family to produce a hardened layer on the surface. During the process, a laser scans across the material, acting as a source, to heat the surface of the material to the austenitization temperature. In the mean time the bulk material acts as a heat sink to cool down the surface rapidly, a thin layer of hardened martensite is formed on the surface [5-6]. The high power density property of the laser leads to a fast thermal cycle and limited energy input that means the final distortion of the workpiece is a minimum and no post-process is needed. The other important property of laser hardening is the self-quenching nature of the process, which allows laser hardening to be integrated in the production line and makes laser hardening a very productive process. Because of these benefits, there are many studies concerned with laser hardening process, *e.g.* Jong-Hyun

* Corresponding author. Tel.: +39-2-2399-8556; fax: +39-2-2399-8585.
E-mail address: anmin.liu@mail.polimi.it.

1875-3892
doi:10.1016/j.phpro.2010.08.166

Hwang [7] had established experiments to treat cast iron piston rings used for marine diesel engines, and G.Duffet [8] had also investigated laser surface treatment on cast iron cylinder bore used for automobile engines by Nd:YAG laser; T. Slatter [9] applied a CO_2 laser to treat the valve seat area of a cast iron cylinder head to improve the wear life of the components.

One well-known problem in laser hardening is the overlapping process [10]. When the surface to be treated is lager than the laser spot a multi-pass strategy is required. In order to get a uniform hardening depth on the surface, an overlapping technique is applied. In the multi-pass hardening processes, the current laser track re-heats the previous one, so the existing martensite is transformed into tempered martensite, which is characterized by lower hardness. The reduction of hardness leads to a lack of uniformity of the mechanical and corrosion resistance properties of the surface [11-13].

In this paper, different process parameters are investigated to optimize a single pass hardening process for grey cast iron in terms of maximum process productivity, once the hardened area depth is fixed. The results are analyzed in terms of depth, microstructure and hardness profile of the hardened zone. Based on these results, the overlapping process is investigated with different overlapping lengths. The microhardness on the surface is tested to evaluate the decrease in the mechanical and wear resistance of the surface due to the back tempering phenomenon.

2. Experimentation design

2.1. Problem definition

The investigated material is a grey cast iron, expressly used in mechanical components where the bulk material has to have high toughness and vibration damping properties, while the surface has to have high wear resistance. These two requirements are usually fulfilled simultaneously by superficial induction hardening of the semi-finished component obtained by casting. Following that the hardened surfaces are grinded in order to match the geometrical requirements. The laser hardening process can be a valid alternative to induction hardening, in particular when the wear resistance properties are ensured by a thin superficial layer, which should be characterized by a very high hardness value. Indicative values resulting from previous experimentations (here not reported for sake of briefness) and from the industrial state of the art show that the minimum depth of the treated area should be around 0.25 mm while a valid reference value for the superficial microhardness value is about 700 HV.

Therefore the experimentation was aimed at defining the process conditions which allow the diode laser to treat the investigated grey iron at maximum process speed, under the constraint that the treated depth has to be more than 0.25 mm as well as the superficial hardness value higher than 700 HV.

2.2. Material

The material used in the experiment was grey cast iron, with the typical pearlite matrix and the graphite flakes shown respectively in Figure 1(a) and (b). The chemical composition and microhardness value of the grey cast iron are listed in Table 1.

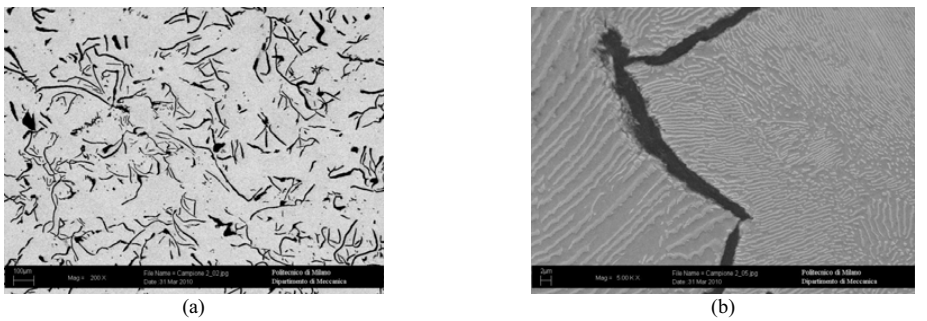

(a) (b)

Fig. 1. SEM images of microstructure of the base material (a) with low and (b) and high magnification

Table 1. Nominal chemical composition (weight %) and the tested hardness of the base material

C	Si	Mn	P	S	Hardness (HV0.3)
3 – 3.2	1.5 – 1.8	0.7 – 0.9	< 0.15	< 0.12	250±13

The melting temperature of the base material was first predicted by evaluating the chemical composition and then was confirmed to be around 1150-1200°C by temperature measurements made with a pyrometer.

2.3. Experimental procedures

A 1000 W continuous wave Rofin DL022 laser (λ=808 nm and 940 nm) was used in the experimentation. In order to achieve the maximum power density on the hardening area, the laser was focused on the material surface. The laser spot has a rectangular form with dimension of 2 mm x 6 mm. No shield gas was applied.

As the melting point of cast iron is lower than pure iron or steel, the feasibility window for hardening is extremely narrow, thus a control system was adopted. The laser was connected to a close-loop measurement and control system, composed of a pyrometer and a PID regulator. The pyrometer measured the thermal radiation from the workpiece surface and then transformed the measured emission to temperature. This measured temperature was compared to a reference value. Then the PID regulator produced a signal used by the laser source to control the power. The surface temperature was kept at the reference temperature by varying the laser power.

Instead of investigating laser powers, different levels of temperature in the feasible hardening window were investigated. The other process variable to be investigated was the scan speed. The experimental set up and the real time measurement and control results are shown in Figure 2. With this measuring and control system, it was possible to control and get a stable temperature on the workpiece surface.

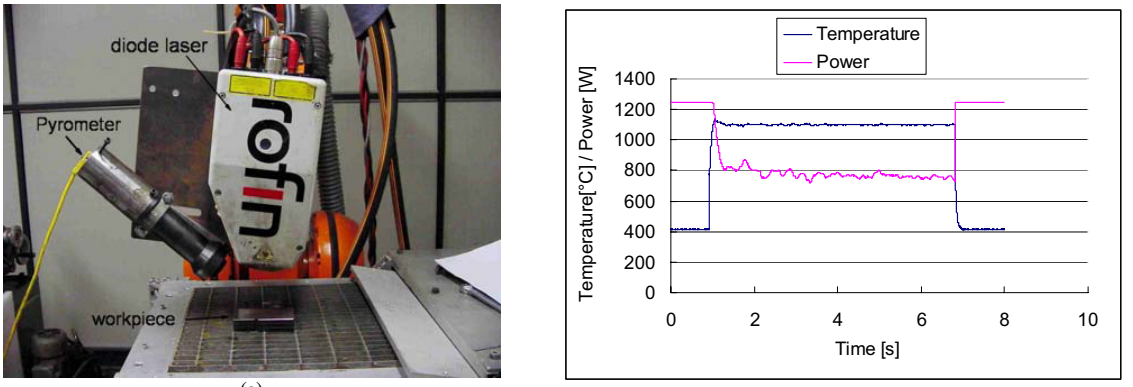

(a) (b)

Fig. 2. (a) Experimental set-up and (b) real time temperature and power measurements

In order to get optimized process parameters for treating a large surface, two experimental campaigns were designed. The first campaign was single pass laser hardening. Independent single passes were executed to understand the effects of different levels of scan speed and temperature on the hardened zone. The temperature and scan speed levels for this campaign are listed in Table 2.

Table 2. Process parameters used in single pass hardening campaign

Temperature on the surface [°C]	1100, 1000
Scan speed [mm/s]	10, 7, 4

For each process condition the temperature values were recorded in real time. Average power was also calculated by averaging the power measurements in the stable phase, *i.e.* for the process shown in Figure 2(b), the averaged

measurements are from 2s to 6s. Calculated average powers for each condition are listed in Table 3.

Table 3. Average power for each process condition

	Scan speed [mm/s]		
Temperature [°C]	10	7	4
1100	834 [W]	770 [W]	614 [W]
1000	743 [W]	665 [W]	567 [W]

After the experiments, sections of the heat treated tracks were made. The samples were ground and polished using common metallographic procedures and etched with 2% Nital reagent for 5-10 seconds. The cross section of the hardened zone was observed with an optical microscope and a SEM. The geometric features of the treated area, width (W) and depth (D), were measured by means of standard image analysis software. Moreover the Vickers microhardness values were measured applying a load of 300 g. The hardness tests were executed along the width direction at a distance equal to 0.15 mm from the top surface and along the depth direction at the centre of the treated area. The geometric features of the hardened zone and hardness test positions are shown in Figure 3.

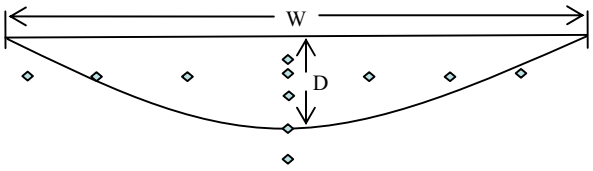

Fig. 3. Cross section dimensions of the laser hardened zone and microhardness test position

The second experimental campaign was multi-pass experiments for treating a large area. Based on the results of single pass hardening, process parameters for overlapping process were set and the overlapping experiments were carried out. From the results of the previous experiment (see further detail in the next section) a temperature of 1100 ºC, with a scan speed 10 mm/s was adopted. A new parameter, “overlapping length (OL)”, shown in Figure 4 was taken into account. To simplify and generalize the process, the calculation of overlapping length was based on considering the width of the hardened zone equal to the laser spot. Four levels of overlapping lengths were adopted: 0.75 mm, 1 mm, 1.25 mm, 1.5 mm. Hardness tests were executed along the width direction on the surface, and in cross section along the depth direction in the overlapping zone (see Figure 4).

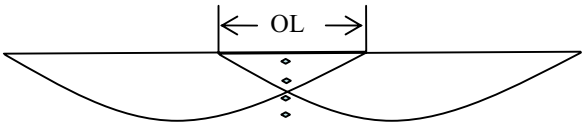

Fig. 4. Overlapping length (OL) in the multi pass process

3. Results and discussion

3.1. Single pass laser hardening

Table 4 shows the typical geometric dimensions of the laser hardened zones. In Figure 5, the experimental results are reported in terms of width and depth as a function of scan speed and surface temperature.

Table 4. Geometric dimensions of laser hardened zone

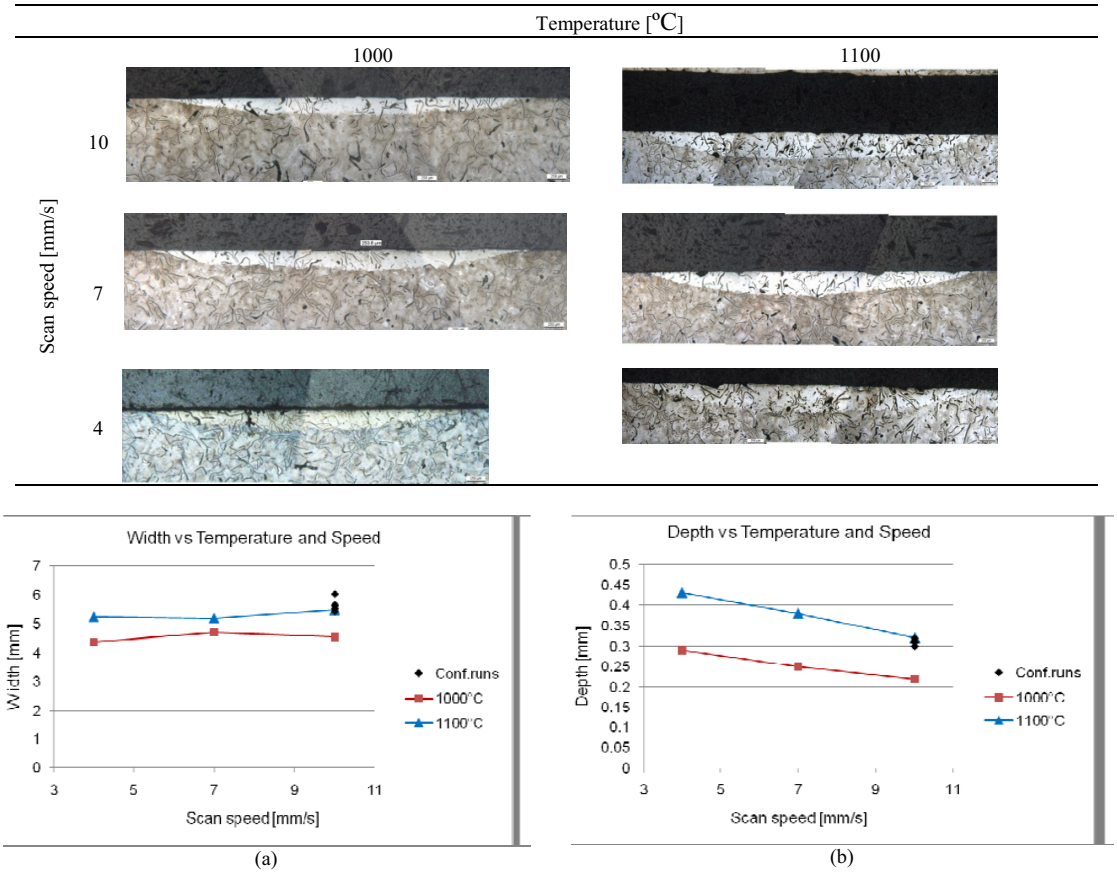

Fig. 5. (a) Hardening width vs temperature and speed and (b) Hardening depth vs temperature and speed

As the Figure 5 shows, the width of the hardened zone is mainly determined by the dimension of the laser spot, while both temperature and scan speed do not affect the width. On the contrary the treated area depth is affected by both parameters: temperature and speed. The best-fit model is linear:

$$D(mm) = -0.875 + 0.00123 \cdot T(°C) - 0.0150 \cdot v(mm/s) \quad (1)$$

The analysis of variance confirmed that the model in Eq.1 is adequate and the adjusted coefficient of determination R^2adj is 97.7%. Residual normality and homogeneity of variance are satisfied. Six confirmation runs executed at the highest speed and temperature confirm the regression model adequacy (see Figure 5(b)). The confirmation runs were executed at the highest temperature and speed because this condition is the set of process parameters that allows the laser to harden at the maximum speed, while the constraint, which is the treated area depth higher than 0.25 mm, is satisfied.

In terms of the temperature values it can be interpreted that higher temperature on the surface means more energy input, which induces a deeper hardened zone. When the temperature on the surface is constant, faster travel speed needs higher laser power and induces a faster thermal cycle that produces a thinner hardened zone. The maximum hardening depth can reach 0.41 mm by keeping the temperature at 1100°C, and scanning the workpiece at the lowest speed 4 mm/s.

Figure 6 (a)-(d) shows the microstructure and microhardness analysis along the depth of the hardened zone. The analysis of results shows that during the laser hardening process, a homogeneous microstructure is obtained in the

hardened zone regardless of the depth.

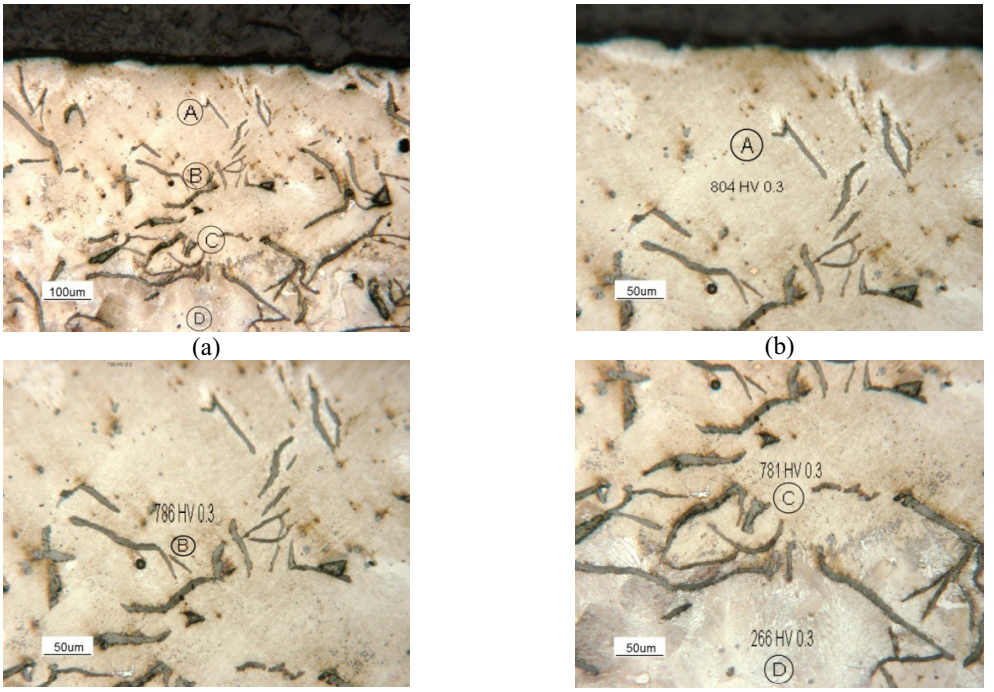

Fig. 6. (a). Microstructure of the hardened zone X100 and (b), (c), (d) microstructure in zone A, B, C, D separately X200

The average hardness was measured to be 700-800 HV and the hardness profiles are reported in Figure 7 and 8. Hardness profiles indicate that the hardness is related neither to the temperature nor to the scan speed. A uniform hardness distribution is obtained in each hardened zone.

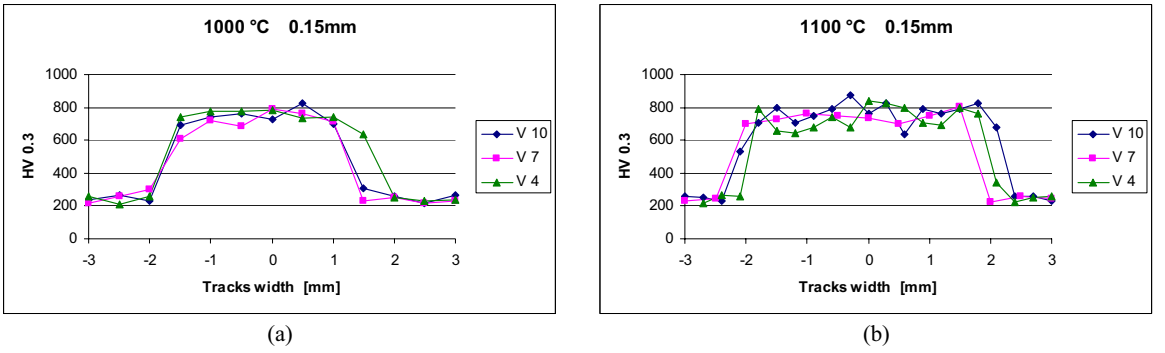

Fig. 7. Hardness profile along the track width

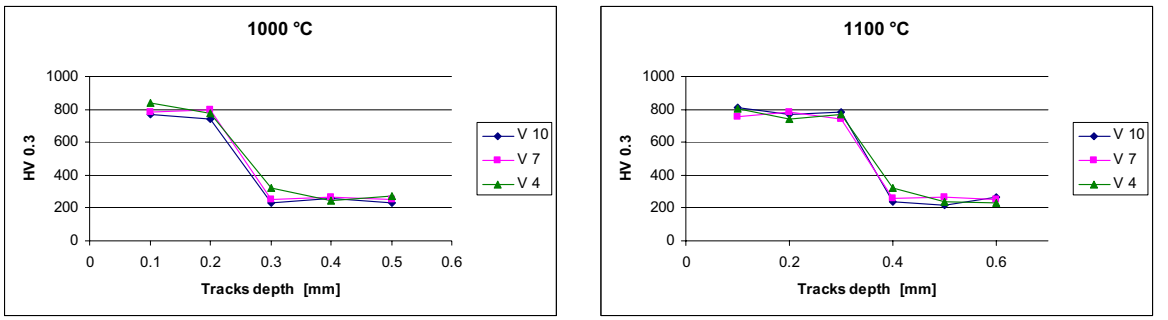

(a) (b)

Fig. 8. Hardness profile along the track depth

The results of the first campaign show that the microstructure and microhardness measurements are independent of the temperature and scan speed; each combination of different levels of temperature and scan speed produces a homogeneous hardened zone and uniform hardness distribution. On the other hand, the depth of the hardened zone is strongly influenced by the investigated parameters.

Therefore the selected optimal condition (T=1100°c and v=10 mm/s) was used in the next campaign aimed at investigating the effect of the overlapping on the treated area properties.

3.2. Multi-pass laser hardening

Since the overlapping process induces two main drawbacks: non uniform surface hardness and non uniform hardening depth, the parameters should be adopted carefully to minimize these drawbacks.

Temperature and scan speed parameters were set as 1100°C and 10 mm/s to get a productive system, after the first experimental campaign. The microstructure of the overlapping zones for different overlapping lengths is reported in Figure 9.

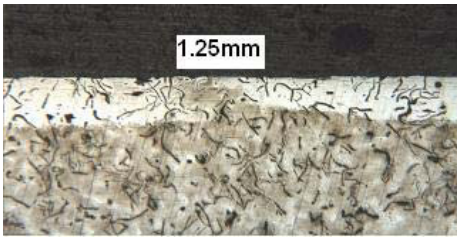

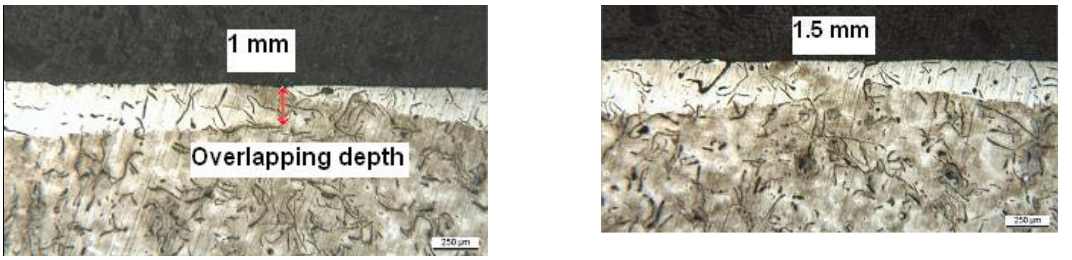

Fig. 9. Microstructure of hardened zone with different overlapping length

The results of overlapping depth measurements are reported in table 5. Only a thin layer is obtained with a small overlapping length equal to 0.75mm; the depth in overlapping zone is only 0.12mm. A constant depth is obtained by adopting larger overlapping length. No significant increase is observed once the overlapping length reaches a certain value starting from the overlapping length of 1 mm.

Table 5. Overlapping length in different overlapping zone

Overlapping length (mm)	0.75	1	1.25	1.5
Overlapping depth (mm)	0.12	0.2	0.24	0.23

The microhardness profiles across the transverse direction are reported in Figure 10. The measurements taken away from the overlapping zones indicate that the hardness on the surface is higher than that in the cross section, *i.e.* between 800HV to 900HV. On the other hand, inside the overlapping zones an abrupt reduction of the hardness values is observed, confirming that the adjacent laser track has been re-heated and the original martensite microstructure has become has been modified.

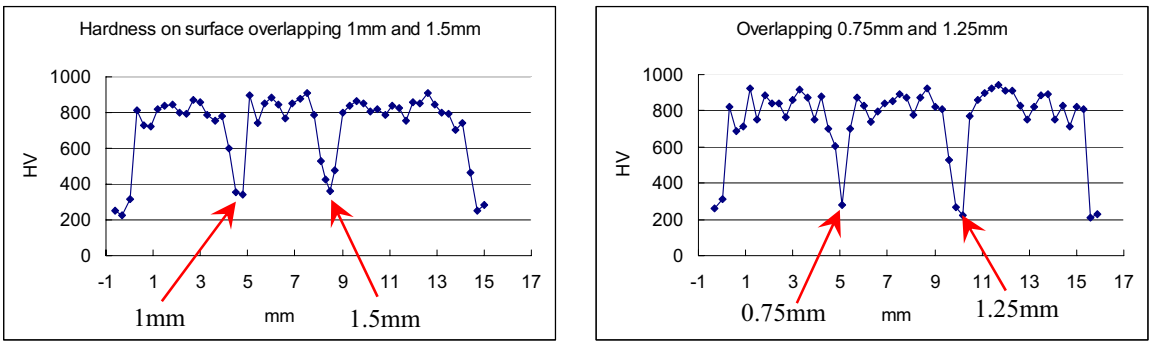

Fig. 10. Hardness profile on the surface of overlapping zone

The corresponding hardness profiles measured inside the overlapping zones are shown in Figure 11. In the back tempered area the reduction of microhardness values is uniform and seems to be not affected by the depth.

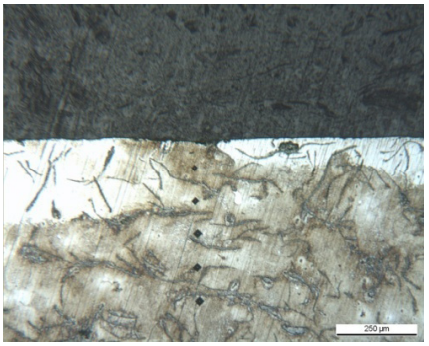

(a)

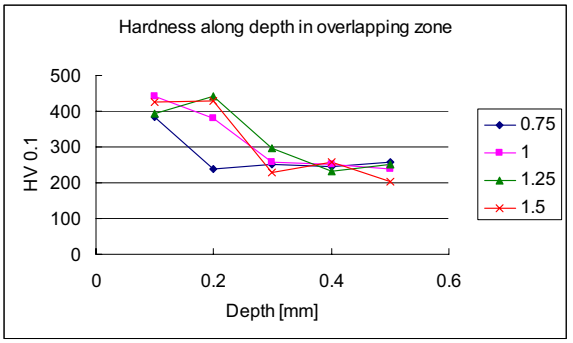

(b)

Fig. 11. Hardness test (a) and hardness profile (b) in overlapping zone

Considering the combination of uniformity of hardening depth and uniformity of hardness, the parameters for the overlapping process can be optimized. Larger overlapping length ensures a uniform hardening depth, but for a given surface, it also means more hardening tracks, this induces a greater overlapping zone with hardness reduction. In case of diode laser hardening with a rectangular laser spot and uniform energy distribution, the depth of the hardening is more uniform than that obtained by other kinds of laser with a Gaussian distribution. In diode laser hardening, when the overlapping length reaches a certain point, the depth in the overlapping zone does not increase significantly, and a uniform hardened zone in depth can be obtained. When the overlapping length exceeds this point, it induces more overlapping zones and hardness reduction. For this experimental campaign, the critical point is 1.25mm. A valid range for overlapping length is from 1 mm to 1.25 mm, which corresponds to 16.7-20.8% of the nominal hardening track width. The process parameters can be selected within this window, based on hardening depth requirements for different applications.

4. Conclusions

Using a control system that is able to modulate the laser power, the effect of surface temperature and scan speed on the results of the hardened layer in terms of geometric characteristics, hardness profile and microstructure were investigated both in single and multi-pass diode laser hardening. In single pass a feasibility window was established to meet the industrial application requirement that the treated area is deeper than 0.25 mm at maximum process speed. A uniform hardened zone can be obtained in single pass laser hardening of grey cast iron with a high power diode laser. Then the condition, which allows the 0.25 mm depth to be obtained at maximum speed, was used to investigate the effect of the multi-pass on the back-tempering treatment experienced by the overlapping area.

The main conclusions of this experimental study are:

1. A homogeneous microstructure is obtained in the laser hardened zone, whose hardness values range from 700 to 800 HV in the cross section, regardless to the temperature and scan speed.
2. The depth of the hardened zone is influenced by both temperature and scan speed. High temperature and slow scan speed mean more energy input that induces a deeper hardened zone. Use of a higher surface temperature, *i.e.* 1100°C, at all the investigated scan speeds produced a hardening layer deeper than 0.3mm. For lower temperature, the depth ranges in the interval 0.2-0.3 mm. The deepest hardening layer was 0.4 mm, obtained at 1100°C and 4 mm/s. Considering productivity and constrains of mechanical applications such as high load, the combination of high temperature and high scan speed (1100°C, 10 mm/s) is the best process parameter condition.
3. An overlapping area, having an extension of about 16.7% to 20.8% of the nominal hardening track width, is an inevitable negative effect when adjacent tracks are investigated. In the overlapping area the micro-hardness values show an abrupt decrease, due to the re-heating of the previous obtained martensite which is tempered. The loss of hardness value is uniform in depth.

Hardness reduction in the overlapping zone is a limit which is difficult to be avoided in the laser hardening of large surfaces. A new approach named Apparent Spot (AS) technique is proposed by the authors in the case of the

hardening of cylindrical surfaces [14]. A high rotation speed is applied to the workpiece during the laser heat treatment. Thus, an apparent spot with homogenous energy distribution is obtained along the circumference. With this technique, by moving the laser along the axis of the workpiece, a uniform hardening surface without overlapping could be obtained.

References

1. Di Flake C. Campbell, Elements of metallurgy and engineering alloys, 453-465
2. M.B. Karamışa, K. Yildizli, Materials Science and Engineering A, 527 (2010) 5225 – 5229
3. Seong-Jun Choo, Sunghak Lee, Soon-Ju Kwon, Metallurgical and materials transactions A, 30A (1999) 1211–1221
4.W.X. Pa, X. Meng, G. Li, Q.X. Fei and C.K. Wu, Surface & Coatings Technology, 197 (2005) 345– 350
5. Kennedy E, Byrne G, Collins D.N, Journal of Materials Processing Technology, 155–156 (2004) 1855–1860
6. John C. Ion, Laser processing of engineering materials, 221-247
7. Jong-Hyun Hwang, Yun-Sig Lee, Dae-Young Kim, Joong-Geun Youn, Materials Engineering and Performance, 11(3) (2002), 294–300
8. G.Duffet, P. Sallamand, A.B. Vannes, Applied Surface Science, 205 (2003) 289–296
9. T. Slatter, H. Taylor, R. Lewis, P. King, Wear, 267 (2009) 797–806
10.G. Tani, L. Orazib, A. Fortunato, CIRP Annals - Manufacturing Technology, 57 (2008) 209 – 212
11. Ritesh S. Lakhkar, Yung C. Shin, Matthew John M. Krane, Materials Science and Engineering A 480 (2008) 209–217
12. Chengwu Yao, BinshiXu, JianHuang, PeileiZhang, Yixiong Wu, Optics and Lasers in Engineering 48 (2010) 20–26
13. J. Grum, R. Sturm, Surface engineering, 21 (2005) 27-34
14. L.Giorleo, A.Liu, B.Previtali, Proceeding of ESAFORM 2010.